Geotechnical Safety and Risk V
T. Schweckendiek et al. (Eds.)

doi:10.3233/978-1-61499-580-7-293

Probabilistic VHM Failure Envelopes for Skirted Foundations in Spatially Variable, Normally Consolidated Clay

T.S. CHARLTON and M. ROUAINIA
School of Civil Engineering and Geosciences, Newcastle University, United Kingdom

Abstract. Skirted foundations are used in offshore applications to resist the large horizontal and moment loads that are characteristic of the ocean environment. The ultimate capacity of a skirted foundation subjected to vertical-horizontal-moment (VHM) loading combinations can be described using failure envelopes in VHM load space. This represents a far more versatile design approach than classical bearing capacity solutions and is able to accommodate complex loading scenarios and similarly complex stress conditions in the soil. Typically, VHM envelopes are constructed using deterministic plastic limit analyses or numerical methods. However, soil is a natural material and as such is inherently variable. The value of soil parameters fluctuates through the ground, as evident in field or laboratory test results. In this study, the ultimate capacity of a skirted foundation in spatially variable undrained clay under VHM loading is investigated. Spatial variation is taken into account using a random field representation of undrained shear strength and the increase of strength with depth typical of a normally consolidated marine clay is considered. The random field is coupled with a finite element method to assess the ultimate limit state. The failure mechanism and ultimate capacity are consequently direct results of the spatial variation of undrained shear strength. Monte Carlo simulation is used to produce probabilistic failure envelopes, based on the probability that the true combination of VHM loads causing failure will fall inside on or inside that envelope. Hence, this method allows designers to select a failure envelope that is associated with an acceptable level of risk.

Keywords. Offshore geotechnics, skirted foundation, failure envelopes, spatial variability, finite element analysis

1. Introduction

In offshore applications, shallow foundations are often equipped with peripheral vertical skirts which penetrate into the seabed. The skirts improve the ability of the foundation to resist the large horizontal and moment loads that are imposed by environmental factors such as wind and waves. In undrained conditions, capacity may be enhanced by the development of suction within the enclosed soil plug which provides short term tensile resistance (Gourvenec, 2007).

The interaction of vertical-horizontal-moment (VHM) loading, shown in Figure 1, is a critical design issue. It has been shown that classical bearing capacity solutions are inadequate for describing the capacity of foundations in complex soil conditions subject to combined VHM loading, and often lead to underprediction of capacity (e.g. Ukritchon et al., 1998; Gourvenec and Randolph, 2003). A far more versatile approach to assessing the ultimate limit state is to construct failure envelopes in VHM load space and compare design loads to those which would lead to failure of the foundation (Randolph and Gourvenec, 2011).

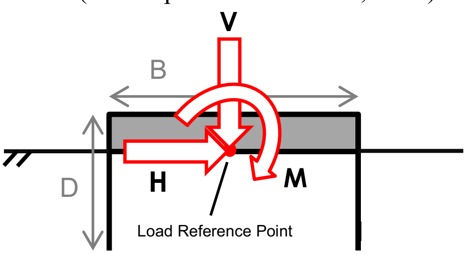

Figure 1. Combined loading of a skirted foundation.

Numerical investigations of the shape of the undrained VHM failure envelope for skirted foundations with various embedment ratios and in uniform and normally consolidated clays have been undertaken by Bransby and Yun (2009) and Gourvenec and Barnett (2011). However, these studies have considered the soil to be described by deterministic parameters following a defined trend across the soil mass. In reality, soil is inherently variable due to complex formation processes and stress history and the values of soil parameters can be observed to fluctuate around a trend (Phoon and Kulhawy, 1999). Uncertainty is therefore intrinsic to geotechnical design, as both loads and resistance are variable.

Reliability methods, such as the first-order reliability method (FORM), can be used to quantify uncertainty at a design point determined by a prescribed limit state function. Partial factors calibrated in this way are recommended for use in classical bearing capacity calculations by many modern design codes, including Eurocode 7 (EC7-1, 2004). The spatial variability of soil properties, and the potential effect on mechanical behaviour, is not considered explicitly.

In this paper, probabilistic VHM envelopes are constructed for a skirted foundation in a spatially variable undrained clay. The probabilistic envelopes are based upon cumulative distribution functions (CDFs), enabling a simple interpretation. In addition, this study incorporates the increase of strength with depth that is typical of marine clays (Randolph et al., 2011) and an important consideration in offshore applications.

2. Methodology

2.1. Overview

The effect of spatial variability on the undrained VHM capacity of a skirted foundation is assessed by coupling a random field model with FE analysis. Monte Carlo simulation is used to characterise the stochastic response, e.g. the probability density function (PDF) of ultimate capacity. The implementation is non-intrusive, meaning the FE code is not modified and proceeds in the usual deterministic manner.

2.2. Simulation of Spatial Variability

The undrained shear strength, s_u, is generally used to determine bearing capacity in undrained conditions. A correlated random field of s_u will therefore be considered to simulate the spatial variability that would likely occur in the field.

Marine sediments are often normally consolidated and exhibit an increasing strength with depth. This creates an additional challenge for simulating spatial variability as the random field can no longer be homogeneous, whereby in the case of a Gaussian random field the mean and variance are constant (Vanmarcke, 2010). An assumption of homogeneity greatly simplifies the treatment of random fields. However, the undrained shear strength may be related to the overconsolidation ratio (OCR) and effective vertical stress (σ'_v) by (Wroth and Houlsby, 1985):

$$\frac{s_u}{\sigma'_v} = r \cdot OCR^m \tag{1}$$

where r and m are constants. In a normally consolidated marine clay, OCR is equal to 1. If a limited mudline strength is accounted for, the profile of s_u increasing with depth may be expressed as:

$$s_u = \mathrm{r} \cdot \gamma' z + s_{u,m} \tag{2}$$

where z is the depth below the mudline and γ' the effective unit weight of the clay. Spatial variability may therefore be taken into account by considering r as a homogeneous random field (Li et al., 2014). Both γ' and $s_{u,m}$ are taken as deterministic quantities.

It is clear that s_u should not be a negative value and a Gaussian distribution would therefore be unsuitable for r. A lognormal distribution takes only positive values, making it an appropriate choice. If $\boldsymbol{x}$ denotes spatial position, the lognormal random field may be generated as follows:

$$r(\boldsymbol{x}) = \exp\left(\mu_{\mathrm{L,r}} + \sigma_{L,r} \cdot G(\boldsymbol{x})\right) \tag{3}$$

$$s_u(\boldsymbol{x}) = s_{u,m} + \gamma' z \cdot r(\boldsymbol{x}) \tag{4}$$

where $G(\boldsymbol{x})$ is a standard homogeneous Gaussian random field of zero mean and unit variance and $\mu_{L,r}$ and $\sigma_{L,r}$ are, respectively, the mean and standard deviation of $ln(r)$.

The standard Gaussian random field $G(\boldsymbol{x})$ is discretised using the spectral representation method, details of which may be found in Shinozuka and Deodatis (1996). Here, an anisotropic exponential autocorrelation function is used. The autocorrelation distances in x- and y-directions (L_x, L_y) of the transformed field $s_u(\boldsymbol{x})$ are equivalent to those of $r(\boldsymbol{x})$ (Wu et al., 2012). The values of L_x and L_y of $ln(r)$ are taken to be 10m and 1m respectively, consistent with reported values in literature (e.g. Lacasse and Nadim, 1996; Phoon and Kulhawy, 1999).

2.3. Finite Element Model

The deterministic simulations are carried out using the commercial FE code PLAXIS 2D (PLAXIS, 2012). A plane strain model of a skirted foundation was created with a typical D/B ratio of 0.25. The clay is assumed to be undrained and obeys a linear elastic-perfectly plastic Mohr-Coulomb constitutive law (equivalent to the Tresca criterion in undrained conditions).

In the deterministic case the undrained shear strength of the clay increases with depth according to $s_u = s_{u,m} + kz$ where k is the increase in s_u per metre depth. A dimensionless parameter, κ, may be used to describe the degree of heterogeneity with $\kappa = kB/s_{u,m}$ (Gourvenec and Barnett, 2011). A value of $\kappa = 2$ was chosen, which corresponds to a fairly typical heterogeneity observed for offshore sediments (see e.g. Andersen et al., 2005). The effective unit weight is taken as 10kN/m^3. In the stochastic case, the mean of s_u is derived from $\mu_r = k/\gamma'$ and the coefficient of variation (COV) of r is chosen to be 0.2, which is based on values of the variability of s_u reported in Lacasse and Nadim (1996).

The FE mesh, consisting of 15-node triangular elements, is shown in Figure 2. The model boundaries are located sufficiently distant to have no effect on the results. Due to the large number of simulations that must be completed, a balance must be found between calculation time and solution accuracy with regards to mesh discretisation. A mesh of 666 elements was found to overestimate uniaxial capacity by no more than 2.5% compared with a mesh of over 2700 elements; this was viewed as acceptable keeping in mind the savings in calculation time.

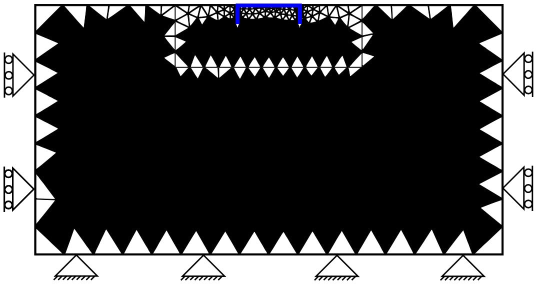

Figure 2. Finite element mesh

The skirted foundation is modelled using rigid plate elements. Interfaces are applied along the vertical skirt with extensions beyond the skirt tip to avoid an unrealistic stress response. It is assumed that suction is generated in the clay plug during loading, thus no reduction in strength is considered between the foundation and soil. Installation effects on the outside wall of the skirt are also neglected.

A load-controlled method is used to define the VHM envelopes. Load probes at different angles, corresponding to fixed load ratios, are applied at the load reference point (Figure 1) until failure. The failure envelope is then constructed from the defined failure points.

3. Results and Discussion

The Monte Carlo procedure involved 1000 random field realisations and subsequent FE analyses. An example of a random field used in the analysis is shown in Figure 3. The increase in s_u with depth can be clearly observed. The autocorrelation distance in the x-direction is an order of magnitude greater than in the y-direction, resulting in horizontal bands of stronger and weaker soil.

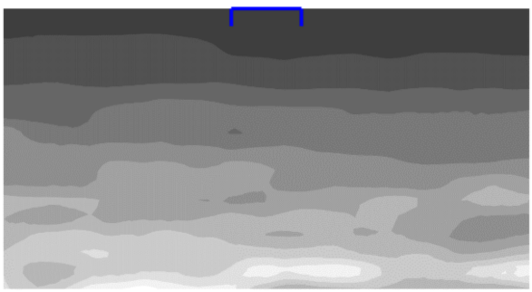

Figure 3. Realisation of a random field of s_u (lighter colour indicates higher s_u).

3.1. Uniaxial Capacity

Figure 4 shows the evolution of the mean and COV of the uniaxial capacities (V_0, H_0 and M_0) throughout the Monte Carlo simulations. The mean is normalised by the respective uniaxial deterministic capacities to facilitate comparison (i.e. $\mu = \mu_Q/Q_{Det}$ if Q is the ultimate capacity for a given load probe). It can be seen that both statistics converge to an approximately constant value. Similar convergence was observed for higher moments (skewness and kurtosis), indicating that after 1000 simulations the response PDF of each load probe has been well captured.

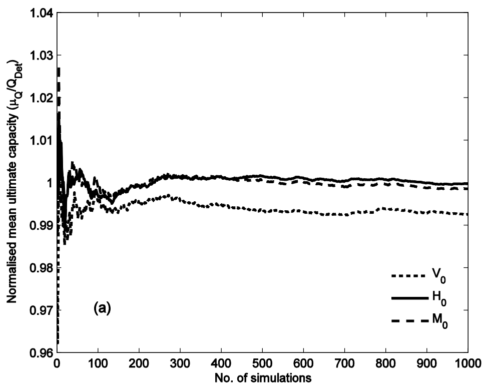

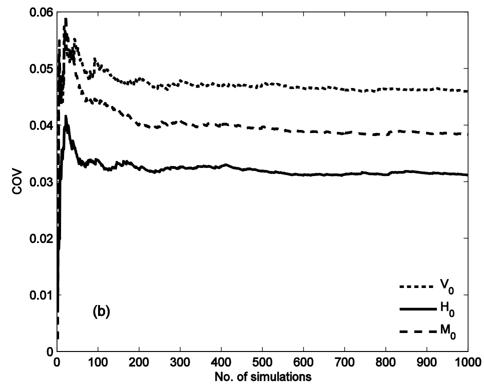

Figure 4. (a) Normalised mean of uniaxial capacities and (b) COV of uniaxial capacities.

The uniaxial bearing capacity factors from stochastic and deterministic analyses are presented in Table 1. For comparison purposes, the reference value of undrained shear strength, $s_{u,tip}$, is taken at skirt tip level. In the stochastic case this corresponds to the prescribed mean value of s_u at that depth, which is equal to the deterministic value.

Firstly, it can be seen that the deterministic FE analysis in this study predicts bearing capacity factors 5-10% less than those reported by Gourvenec and Barnett (2011). It is notable that both the mean horizontal and moment bearing capacity factors are equal to the deterministic value, whereas the vertical capacity factor is approximately 1% lower. As evident in the values of COV shown in Figure 4(b), the variability of the vertical capacity factor is also the highest.

Table 1. Stochastic and deterministic uniaxial bearing capacity factors.

	Mean	Standard deviation	Deterministic	Gourvenec & Barnett (2011)
$V_0/Bs_{u,tip}$	8.53	0.39	8.59	9.02
$H_0/Bs_{u,tip}$	2.05	0.06	2.05	2.15
$M_0/B^2s_{u,tip}$	1.03	0.04	1.03	1.14

3.2. Probabilistic VHM Failure Envelopes

The failure envelopes from each Monte Carlo simulation are shown in Figure 5, in addition to the deterministic envelopes. Consideration of the spatial variability of s_u has the potential to result in significant divergence of the failure envelope from the deterministic solution. For the VH and VM envelopes, the stochastic capacity can vary up to +/- 20% of the deterministic. In the HM plane, the variability of the response is asymmetric. There is significantly more variability for combinations of negative horizontal load and moment than for positive horizontal loads.

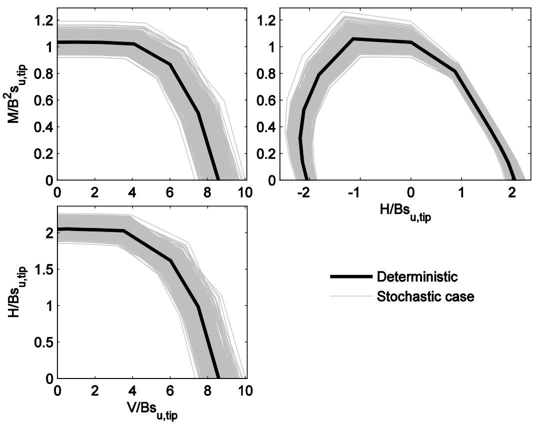

Figure 5. Stochastic and deterministic VHM failure envelopes.

Whilst it is clear from Figure 5 that consideration of spatial variability has the potential to affect the size and shape of the failure envelopes, it would be useful to quantify this variability in capacity in order to use the envelopes in design. This may be achieved by observing that the capacity in each load probe direction is a random variable, denoted Q. The results of the Monte Carlo simulation represent samples from the unknown PDF of each load probe. The CDF of each load probe, F_Q, is used to define the probabilistic envelopes, allowing for a simple interpretation. To create a probabilistic failure envelope, it is necessary to obtain a capacity Q_p such that for a given probability p:

$$p = F_Q(Q_P) = P(Q \leq Q_P) \tag{5}$$

so,

$$Q_p = F_Q^{-1}(p) \tag{6}$$

The probabilistic failure envelope for p is therefore the envelope on which there is a probability p that the ultimate capacity of the foundation will occur *on or inside* that envelope. Hence, a suitable value of p for design might be 5% for example.

Cassidy et al. (2013) constructed probabilistic failure envelopes by ordering a cluster of failure points and using an empirical estimate of the CDF. However, to obtain unique values of Q_p using Eq. (6), the CDF must be a continuous and strictly increasing function. This makes the empirical CDF unsuitable, particularly at the tails of the distribution, where samples are necessarily limited. Here, kernel density estimation (KDE) (Botev et al., 2010) is used to estimate the CDF, producing a smooth function that can be inverted. This is illustrated in Figure 6, which shows the CDF of the horizontal bearing capacity factor estimated empirically and by KDE.

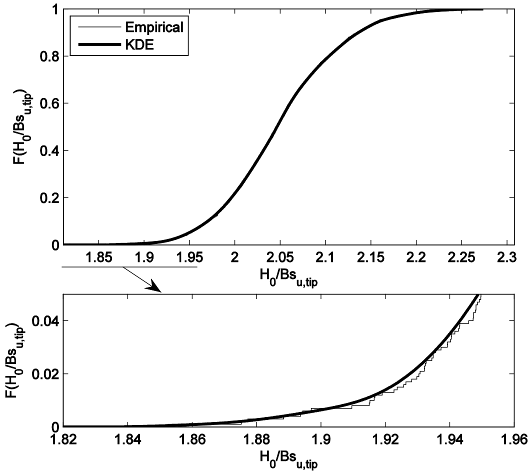

Figure 6. CDF of horizontal bearing capacity factor

A non-parametric technique is applied as it is assumed that nothing is known about the response prior to analysis. As no closed-form expression is available, values of the CDF are evaluated on a fine grid (at 4096 points) and interpolation used to solve Eq. (6).

The probabilistic VHM failure envelopes are presented in Figure 7. The probabilistic envelopes are a similar shape to the deterministic envelope suggesting the CDF of each load probe is relatively consistent. This may be due to only one stochastic soil parameter being considered.

The median (50%) envelope can be seen to be very close to the deterministic. If the simple design process outlined in section 1 were followed only considering the deterministic envelope, the probability that the actual capacity would be less than envisaged is approximately 50%. This may be unacceptably high, and demonstrates the importance of including the spatial variability of soil parameters in design.

The probabilistic failure envelopes offer a simple quantification of the uncertainty in ultimate capacity, allowing designers to select a failure envelope that corresponds to a given level of risk. It is important to note that the envelopes shown in Figure 7 are applicable only to the specific foundation considered. Changes in, for example, autocorrelation distance or COV would alter the size and shape of the envelopes.

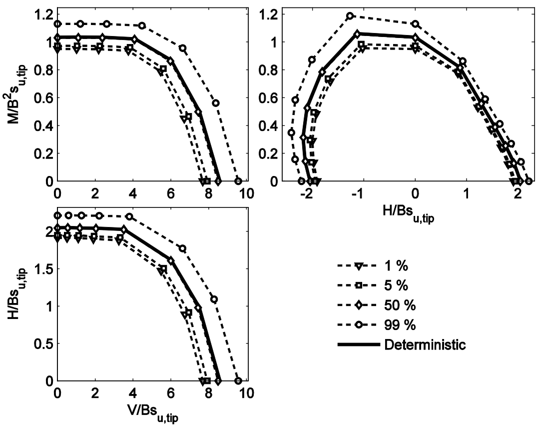

Figure 7. Probabilistic VHM failure envelopes.

4. Conclusions

This study has presented probabilistic VHM failure envelopes for a skirted foundation in spatially variable clay. The increase in undrained shear strength with depth commonly observed in marine clays has been taken into account by a transformation of a homogeneous random field. Monte Carlo simulations employing an unmodified FE code were used to characterise the stochastic response, with VHM capacity being determined by load probes of fixed load ratio. The probabilistic failure envelopes were constructed by estimating the CDF of each load probe using a non-parametric KDE method. This avoids making assumptions about the response prior to analysis whilst producing accurate failure envelopes and simplifying interpretation.

By taking into account the spatial variability of the undrained shear strength, the probability of the ultimate capacity being less than that predicted in a deterministic analysis is approximately 50%. This illustrates the importance of quantifying the effects of the spatial variability of soil parameters. The probabilistic envelopes presented here are limited to the specific case considered, however the methodology demonstrates a straightforward and effective way of quantifying and understanding uncertainty in ultimate limit state design.

Acknowledgements

The first author is funded by a studentship from the Engineering and Physical Sciences Research Council (EPSRC) and Atkins. This support is gratefully received and acknowledged. The authors would also like to thank Dr Paul Bonnier for his assistance with PLAXIS 2D.

References

Andersen, K. H., Murff, J. D., Randolph, M. F., Clukey, E. C., Erbrich, C. T., Jostad, H. P., Hansen, B., Aubeny, C., Sharma, P., and Supachawarote, C. (2005). Suction anchors for deepwater applications', *International Symposium on Frontiers in Offshore Geotechnics (ISFOG)*, Perth, Balkema, 3-30.

Botev, Z. I., Grotowski, J. F., and Kroese, D. P. (2010). Kernel density estimation via diffusion, *Annals of Statistics*, **38**(5), 2916-2957.

Bransby, M. F., and Yun, G. (2009). The undrained capacity of skirted strip foundations under combined loading. *Géotechnique*, **59**(2), 115-125.

Cassidy, M. J., Uzielli, M., and Tian, Y. (2013). Probabilistic combined loading failure envelopes of a strip footing on spatially variable soil, *Computers and Geotechnics*, **49**, 191-205.

EC7-1 (2004). *Eurocode 7: Geotechnical design – Part 1: General rules, BS EN 1997-1:2004,* British Standards Institution, London.

Gourvenec, S., and Randolph, M. (2003). Effect of strength non-homogeneity on the shape of failure envelopes for combined loading of strip and circular foundations on clay, *Géotechnique*, **53**(6), 575-586.

Gourvenec, S. (2007). Failure envelopes for offshore shallow foundations under general loading, *Géotechnique*, **57**(9), 715-728.

Gourvenec, S., and Barnett, S. (2011). Undrained failure envelope for skirted foundations under general loading. *Géotechnique*, **61**(3), 263-270.

Lacasse, S., and Nadim, F. (1996). Uncertainties in Characterising Soil Properties, *Uncertainty in the Geologic Environment*, ASCE, New York, 49-75.

Li, D. Q., Qi, X. H., Phoon, K. K., Zhang, L. M., and Zhou, C. B. (2014). Effect of spatially variable shear strength parameters with linearly increasing mean trend on reliability of infinite slopes, *Structural Safety* **49**, 45-55.

Phoon, K. K., and Kulhawy, F. H. (1999). Characterization of geotechnical variability, *Canadian Geotechnical Journal*, **36**(4), 612-624.

PLAXIS (2012). *PLAXIS 2D 2012*, Plaxis bv, Delft, Netherlands.

Randolph, M. F., Gaudin, C., Gourvenec, S. M., White, D. J., Boylan, N., and Cassidy, M. J. (2011). Recent advances in offshore geotechnics for deep water oil and gas developments, *Ocean Engineering*, **38**(7), 818-834.

Randolph, M. F., and Gourvenec, S. (2011). *Offshore geotechnical engineering*, Spon Press, London.

Shinozuka, M., and Deodatis, G. (1996). Simulation of multi-dimensional Gaussian stochastic fields by spectral representation, *Applied Mechanics Review*, **49**(1), 29-53.

Ukritchon, B., Whittle, A. J., and Sloan, S. (1998). Undrained limit analyses for combined loading of strip footings on clay, *Journal of Geotechnical and Geoenvironmental Engineering*, **124**(3), 265-276.

Vanmarcke, E. (2010). *Random Fields: Analysis and Synthesis*, World Scientific, Singapore.

Wroth, C. P., and Houlsby, G. T. (1985). Soil Mechanics – Property Characterization and Analysis Procedures, Keynote Lecture, *Proc. 11th Int. Conf. on Soil Mechanics and Foundation Engineering (ICSMFE)*, San Francisco, 1-55.

Wu, S. H., Ou, C. Y., Ching, J., and Juang, C. H. (2012). Reliability-based design for basal heave stability of deep excavations in spatially varying soils, *Journal of Geotechnical and Geoenvironmental Engineering*, **138**(5), 594-603.